The Application of General Circulation Models to the Atmospheres of Terrestrial-Type Moons of the Giant Planets

I. C. F. Müller-Wodarg

Atmospheric Physics Laboratory, University College London, United Kingdom and
Center for Space Physics, Boston University, Boston, MA

General Circulation models are for the first time applied to the upper atmospheres of Saturn's moon Titan and Neptune's moon Triton. Calculations reveal that solar driven day-night temperature differences are during solar maximum (minimum) around 20 (10) K on Titan and 1.5 (0.6) K on Triton, with day to night horizontal winds of up to 60 (30) m/sec on Titan and 3 (1) m/sec on Triton. Analysis of the heating terms reveals that solar heating is balanced primarily by vertical conduction on both moons and in addition by HCN rotational line cooling on Titan. Adiabatic processes are shown to be important in reducing the day-night temperature differences. The thermospheres of both moons extend into space by around 30% of the moons' radii, enhancing not only the vertical winds and adiabatic processes, but also high latitude nightside solar heating. This is particularly significant on Titan and implies that nighttime temperatures poleward of 60° differ little from the dayside values, with important implications on the global dynamics. Analysis of acceleration terms shows that dynamics driven by solar heating are characterized by the balance between pressure gradients and viscous drag. On Titan, curvature forces and horizontal advection play an important role as well. Geostrophic balance does not apply on either of the moons. Effects of energetic coupling to the magnetospheres of Saturn and Neptune and coupling to lower atmospheric waves and winds are predicted to be potentially important in altering temperatures and dynamics.

1. INTRODUCTION

Our solar system consists of nine planets which are orbited by at least 90 natural satellites. The moons may be divided according to their sizes into three different categories, those with radii larger than around 1000 km; those with radii ranging from around 100 to 1000 km and, thirdly, those smaller than 100 km which are mostly irregularly shaped. Given that our own moon has a radius of 1700 km, the first category are referred to as "terrestrial type moons". Apart from our own, all other of the 7 terrestrial-sized moons are located in the outer parts of our solar system, orbiting planets Jupiter, Saturn and Neptune. The Earth's moon and Jupiter's Ganymede, Io, Europa and Callisto are surrounded by thin transient gas layers, as discussed in Chapters III.2 and III.3 of this monograph. In contrast, the other two terrestrial-type moons, Saturn's Titan and Neptune's Triton possess non-transient (permanent) atmospheres.

Titan, located at 9.5 A.U. distance from the Sun, was discovered in 1655 by Dutch astronomer Cristiaan Huygens. It is after Ganymede the second-largest moon in our solar system, around 40% the size of Earth and larger than planet Mercury. Titan, like Venus, is permanently covered by a thick global layer of clouds, obscuring any surface features from our view. Triton is almost half the size of Titan and slightly smaller than the Earth's moon. Given its small size and large distance from the Sun of 30 A.U., Triton was discovered only in 1846 by British astronomer William Lassel and is the only moon in our solar system to orbit a planet in retrograde direction, opposite to the planet's rotation. As our own moon, Titan and Triton orbit their mother planets at the same rate as they rotate, so the same side of their surfaces always faces the planet.

This Chapter presents calculations of global wind and temperature profiles in the upper atmospheres of Titan and Triton, using general circulation models (GCM's). Similar models have proven to be very useful in understanding the behavior of the Earth's and other planetary atmospheres (see Chapters IV.1, IV.2). Section 2 gives a historical overview of milestones in the exploration of Titan's and Triton's atmospheres and lists key properties. Section 3 is a brief description of the GCM codes and Section 4 presents the results from calculations. Section 5 discusses coupling of the thermospheres to regions above and below, while Section 6 summarizes the findings.

2. ATMOSPHERIC STRUCTURE AND COMPOSITION

2.1. Titan

The atmosphere of Titan has some remarkable similarities with that of Earth, prompting the idea that Titan may resemble the Earth's atmosphere during its early pre-biotic development stages. The surface pressure on Titan is surprisingly high at around 1.6 bar, 60% larger than that on Earth, and the primary atmospheric gas is N_2, followed by hydrocarbons, mostly CH_4. Due to the smaller mass and radius of Titan, gravity is smaller than on Earth and hence the atmosphere more extended. Calculations in Section 4 will show that the extended nature of the atmosphere has important consequences for the gas behavior.

Most of our current knowledge about Titan was provided by the remote sensing experiments during the Voyager 1 and 2 flybys in November 1980 and August 1981, respectively. The atmospheric thermal structure below 200 km was measured by the radio occultation experiment (RSS), infrared interferometer spectrometer (IRIS) and ultraviolet spectrometer (UVS) of Voyager 1 in November, 1980 (*Lindal et al.*, 1983; *Lellouch et al.*, 1989; *Yelle et al.,* 1997), while the thermal structure above 500 km was derived both from the ultraviolet solar occultation experiment of UVS (*Smith et al.*, 1982) and the IRIS measurements on Voyager

2 in August, 1981 (*Letourner and Coustenis*, 1993). In their analysis of the UVS data, *Smith et al.* (1982) determined an exospheric temperature of 185±20 K, a CH_4 mole fraction of 8±3 % and a C_2H_2 mole fraction of around 1%. This pioneering investigation represented the first direct measurement of the composition of Titan's atmosphere and, along with the results from the radio occultation (*Lindal et al.*, 1983) and infrared observations (*Hanel et al.*, 1981), the first direct measurement of the temperature of Titan's atmosphere. Subsequently, *Strobel et al.*, (1992) pointed out apparent inconsistencies in the determination of CH_4 densities by *Smith et al.* and suggested a significantly lower mole fraction. A comprehensive analysis by Vervack et al. (2001) finds CH_4 and C_2H_2 mole fractions smaller than the results by *Smith et al.* and an exospheric temperature of 150±3 K, nearly 25 K cooler. Thus there remains some ambiguity about exospheric temperatures and some of the mole fractions. Further important information about Titan's atmosphere was provided by the occultation of 28 Sgr in July 1989 which allowed the derivation of temperature, pressure, haze optical depth and zonal velocities as a function of latitude and altitude in the 250 to 450 km height regime (*Hubbard et al.*, 1993). These observations suggested the presence of strong zonal jets in Titan's stratosphere and lower mesosphere with peak velocities of around 150 m/sec. These super-rotating jets may have important implications on the dynamics in the thermosphere, as discussed in Section 5. Strong jets are also found on Venus and Mars, as discussed in Chapter III.1.

Considerable advances in the exploration of Titan are expected from the forthcoming Cassini/Huygens mission, due to arrive at the Saturnian system in July 2004. The mission involves two spacecrafts, the Cassini orbiter and Huygens probe. The latter will enter Titan's atmosphere around January 2005 and, while parachuting to Titan's surface, retrieve a 1-dimensional profile of atmospheric parameters in the troposphere and stratosphere below 250 km altitude. In contrast, Titan's thermosphere will be explored by the Cassini orbiter throughout its anticipated lifetime of 4 years. On its orbit around Saturn, the Cassini spacecraft will dive into Titan's upper atmosphere, reaching down to altitudes of 950 km, and retrieve in-situ neutral and ion composition, temperatures and dynamics.

One-dimensional models for the thermal structure of Titan's upper atmosphere were presented by *Friedson and Yung* (1984), *Lellouch* (1990) and *Yelle* (1991). These models were constrained by Voyager data, primarily the solar occultation experiment observed with the ultraviolet spectrometer, and gave a comprehensive insight into the composition and energy sources and sinks. The models suggest Titan's thermosphere to be heated primarily by absorption of solar EUV radiation through N_2 and CH_4 and cooled by radiative emissions in the rotational bands of HCN as well as downward molecular conduction. Some analyses

of Voyager data inferred unusually large values for the eddy mixing coefficient of up to 10^8 cm^2/sec (*Strobel et al.*, 1992), indicating either unusually strong turbulent mixing on Titan or effective vertical transport of constituents. One-dimensional models do not calculate winds and thus cannot account explicitly for their effects on composition. Estimates of dynamics in Titan's thermosphere were presented by *Rishbeth et al.* (2000) through scale analysis of the equations of motion. First self-consistent calculations of dynamics in Titan's thermosphere were presented by *Müller-Wodarg et al.* (2000), using a global general circulation model. These calculations will form the basis for discussions in Section 4.

Titan orbits the Sun once every 29.5 years, spanning the duration of more than 2 solar cycles. As described earlier, the key observations were made in 1980/1981 and 1989, with Cassini observations due to take place between 2004 and 2008, almost one Titan year after the first observations. Figure 1 a) shows the change of Titan's sub-solar latitude with time between 1975 and 2010, with the observation dates and changes in solar activity indicated. The figure illustrates that Voyager measurements were made close to equinox conditions at solar maximum, while the Cassini mission will encounter late southern hemisphere summer to spring conditions at low to medium solar activity levels.

2.2. Triton

Not much was known about Neptune's largest moon Triton before the Voyager 2 flyby in summer 1989, including such fundamental parameters as mass, radius and surface albedo. Earlier ground-based observations of solar reflection spectra had already indicated the presence of surface ices on Triton, predominantly N_2 and trace amounts of CH_4 and CO (*Cruikshank and Silvaggio*, 1979), findings which were confirmed by Voyager data (*Cruikshank et al.*, 1993; *Owen et al.*, 1993). The atmosphere of Triton is considerably thinner than that of Titan, with a surface pressure of around 14 μbar (*Gurrola et al.*, 1991). Triton's atmosphere is believed to be in vapor pressure equilibrium with the surface ices, so it is maintained at a constant temperature by the surface ice through processes such as condensation and sublimation (*Trafton*, 1984; *Ingersoll*, 1990; *Yelle et al.*, 1995). This assumption constrains the one-dimensional models of vertical temperature and pressure profiles with the atmospheric measurements.

Temperature and pressure profiles were measured between the ground and 50 km altitude by the Voyager radio occultation experiment (RSS) (*Gurrola et al.*, 1991) and infrared interferometer spectrometer (IRIS) (*Conrath et al.*, 1989) and between 450 and 700 km altitude by the ultraviolet spectrometer (UVS) solar occultation experiments (*Broadfoot et al.*, 1989; *Krasnopolsky et al.*, 1993). Temperature is believed to initially decrease with altitude from its surface value by up to 1 K near 8 km height, the

tropopause (*Yelle et al.*, 1991), and then increase to the exospheric value. The IRIS and UVS observations suggested temperature values of 38±3 K on the daytime surface, of 40±5 K between 0 and 50 km and exospheric values of 102±3 K between 450 and 700 km altitude. Models by *Strobel and Summers* (1995), *Krasnopolsky et al.* (1993) and *Strobel et al.* (1996) were constrained by these Voyager data and the studies by *Stevens et al.* (1992) suggested principal energy sources on Triton to be solar EUV absorption and precipitating electrons from Neptune's magnetosphere. The importance of magnetospheric heating on Triton is further discussed in Section 5. *Krasnopolsky et al.* (1993) determined N_2 densities of 1×10^{15} cm^{-3} at the bottom of the thermosphere and *Strobel and Summers* (1995) derived CH_4 densities of 1×10^{11} cm^{-3} which become negligible at around 150 km altitude. It follows that maximum CH_4 mixing ratios on Triton are around 1×10^{-4}, considerably smaller than on Titan. Voyager UVS occultation data also suggested the presence of CH_4 haze particles in Triton's lower atmosphere (*Smith et* al., 1989; *Herbert and Sandel*, 1991) which may result from condensation of CH_4 photolysis products such as C_2H_4 (*Strobel et al.*, 1990). While N_2 and CH_4 were directly detected by the Voyager UVS solar and stellar occultations, only upper limits could be given for the CO abundance. The value has been subject of controversy, with estimates ranging from 0.01 (*Broadfoot et al.*, 1989) to 10^{-3} (*Strobel and Summers*, 1995) and 3×10^{-4} (*Stevens et al.*, 1992). Given that CO is an effective radiative coolant this value is of some importance when determining the energy loss processes in Triton's thermosphere.

First Earth-based data for the 20-100 km height regime were obtained from ground-based observations of stellar occultation in July 1993 (Tr60) and August 1995 (Tr148) (*Olkin et al.*, 1997) as well as July 1997 (Tr176) (*Elliot et al.*, 2000a) and, from the Hubble Space Telescope, in November 1997 (Tr180) (*Elliot et al.*, 1998; 2000b). These observations allowed detection of possible trends with time of the pressure and temperature values which could indicate seasonal changes. Given its long orbital period around the Sun (165 years), any seasonal changes on Triton over a few years are expected to occur slowly, and comparing Voyager observations to the stellar occultations of Tr60 and Tr148 indicated no clear trend beyond data accuracy. The Hubble Space Telescope observations of the Tr180 occultation however suggested that surface pressure had risen since the time of Voyager observations (*Elliot et al.*, 2000b), suggesting a warming of the N_2 surface frost. This trend is supported by the Tr176 occultation results (*Sicardy et al.*, 1998; *Elliot et al.*, 2000a). Triton reached southern hemisphere solstice (-49°87' sub-solar latitude) in September 2000, so a heating of the surface between 1989 and 1997 could suggest a larger concentration of N_2 ice at higher latitudes, which are illuminated strongest during solstice. Figure 1 b) illustrates the change of Triton's sub-solar

latitude between 1975 and 2010 as well as the times of key observations. The figure illustrates that the occultation of Tr180 is most suitable for comparison with Voyager data since it occurred at roughly the same (high) level of solar activity, while all other occultations occurred closer to solar minimum conditions.

Several of the Voyager observations suggested the presence of strong lower atmosphere winds on Triton (*Smith et al.*, 1989; *Hansen et al.*, 1990; *Soderblom et al.*, 1990), which could be caused by N_2 maintaining vapor pressure balance with the surface ice (*Ingersoll*, 1990) or by uneven surface heating of frost and dark areas (*Elliot et al.*, 2000b). Ground-based observations of Tr60, Tr148 and Tr176 suggested a significant deviation of Triton's atmosphere from circular shape near 20 km altitude. One plausible explanation for this elliptical shape could be the presence of supersonic winds (280 m/sec, compared with a sound speed of 140 m/sec) in Triton's lower and middle atmosphere (*Elliot et al.*, 1997; *Elliot et al.*, 2000a), but since equator-to-pole variations of pressure at fixed altitude are of the same magnitude as the pressure itself, the elliptical shape is an unlikely permanent state of the atmosphere. Also, the non-spherical shapes during the Tr148 and Tr176 occultation were inconsistent with each other in terms of size and orientation (*Elliot et al.*, 2000a), so the strong jets on Triton and elliptical shape of its atmosphere are to-date still unresolved problems.

3. THE GENERAL CIRCULATION MODELS

The aim of our calculations is to compare the basic solar-driven dynamics and global temperature profiles on Titan and Triton and to understand their differences. Therefore, the types of models used here are general circulation models (GCM's). Two versions of the same GCM were used which differed only in the fundamental parameters summarized in Table 1. The calculations were carried out on a spherical co-rotating Eulerian pressure coordinate system with fully flexible spatial and temporal resolutions which were set to 6° (latitude) by 18° (longitude) by 0.5 scale height (vertical), using a time step of 10 seconds. In essence, the two GCM's solve self-consistently the 3-dimensional time-dependent Navier-Stokes equations of energy, momentum and continuity by explicit time integration, taking into account external heating by solar EUV radiation. Solar EUV heating rates are calculated by integration of heating rates along the ray paths through the atmosphere. For Titan, the model also considers cooling in the rotational bands of HCN with full calculations of radiative transfer. Although CO and CH_4 cooling is thought to be present on Triton as well, it is in the thermosphere much less important than the HCN cooling on Titan and therefore ignored in these calculations. Other terms in the energy equation are molecular conduction, advection and adiabatic heating and cooling. The momentum equation

used in both GCM's considers pressure gradients, Coriolis forces, advection, viscosity and curvature forces which arise from the gases moving along a sphere. A detailed description of the GCM for Titan, including a thorough discussion of the energy and momentum equation terms was given by *Müller-Wodarg et al.* (2000). Default boundary conditions are zero vertical gradients of temperature and winds at the top boundary and globally constant temperatures with vanishing winds at the bottom boundary. In Section 5, the implementation of winds at the lower boundary is discussed in order to account for dynamical coupling to lower heights. For Titan, the three constituents N_2, CH_4 and HCN are considered, with the former two being the main absorbers of solar EUV radiation and thus responsible for the solar heating input, while the latter, as discussed previously, is an important radiative coolant. Photochemistry and gas diffusion are not calculated here, the constituent mixing ratios are kept globally constant on pressure levels. First results from a recently developed version of the Titan GCM which calculates self-consistently the 3-component gas diffusion (*Müller-Wodarg and Yelle*, 2001) have shown that inclusion of gas diffusion has a small influence on the temperature structure and dynamics, increasing the day-night temperature gradient by 10 K at most and reducing the horizontal wind speeds by up to 10 m/sec. Ignoring photochemistry on Titan is a valid approximation for the purpose of these calculations since we are primarily interested in diurnal features and photochemical lifetimes of N_2 and CH_4 in the height regime of interest are longer than a Titan day. Gas mixing ratios in the Titan GCM are here taken from the model by *Yung et al.* (1984), while for Triton we assumed a globally constant height-independent N_2 mixing ratio of 99.99 % and CH_4 mixing ratio of 0.01 %, based on the values by *Krasnopolsky et al.* (1993) and *Strobel and Summers* (1995).

4. SOLAR DRIVEN DYNAMICS AND TEMPERATURES

4.1. Global Structures

Figure 2 shows global profiles of exospheric temperatures and horizontal winds on Titan and Triton for equinox and southern hemisphere solstice conditions, as calculated by the GCM's. Equinox simulations were carried out at solar maximum, while the solstice runs assumed solar minimum, thus mimicking seasonal and solar conditions encountered on Titan by Voyager and Cassini, respectively (see Figure 1 a). Values in Figure 2 are shown as profiles versus latitude and local time. For convenience, the days were subdivided into 24 intervals, each interval corresponding to 15.8 h on Titan (one "Titan hour") and 5.6 h on Triton (one "Triton hour"). Note that in the interest of direct comparison between the two moons Figure 2 shows temperatures and winds driven by

solar heating alone. Discussions in Section 5 will show that dynamical coupling to lower altitudes and energetic coupling to the magnetospheres of Saturn and Neptune are also likely to affect the temperatures and winds. Nevertheless, it is important to be able to separate out the solar-driven component, so in the following we concentrate on that one.

The simulations shown in Figure 2 illustrate the following basic differences between the two moons: (a) Solar driven exospheric temperatures on Titan reach 178 (157) K at solar maximum (minimum), those on Triton reach 53 (44) K. Note that for Triton the measured values are 102 K (see 2.2) and the additional heating source are believed to be precipitation of magnetospheric electrons (*Stevens et al.*, 1992, see also Section 5). The solar-driven exospheric temperatures for Titan are in good agreement with measurements, suggesting that solar radiation provides the principal energy source there. On Titan, the globally averaged temperature at the base of the thermosphere for solar maximum (minimum) is around 140 (135) K. On Triton we assume a value of 40 K both at solar maximum and minimum. Exospheric values in the GCM calculations are reached near the 10 *n*bar (1200 km) level on Titan and 1 *n*bar (370 km) level on Triton. Note that values of heights associated with the pressures for Triton are lower in our simulations, compared to Triton's real atmosphere, due to the smaller temperature values calculated by the GCM. (b) Day-night temperature differences on Titan are 20 (10) K at solar maximum (minimum), corresponding to 11 (6)% of the background values. Those on Triton are 1.5 (0.6) K, or 3 (1)%. For comparison, day-night thermospheric temperature variations are on average around 25% on Earth, 40% on Mars and 80% on Venus (see Chapter IV.1 and *Bougher et al.*, 1999). The reason for the considerably smaller day-night differences on Triton is that solar heating there is considerably weaker than on Titan by a factor of 100 and its rotation rate around 3 times faster. Discussions of heating terms in Section 4.3 will show that adiabatic dayside cooling and nightside heating contribute towards reducing the day-night temperature differences on both moons. Adiabatic processes are important on Mars as well, due to its small radius, but less on Earth and Venus (see Chapter IV.1 and *Bougher et al.*, 1999; *Bougher et al.*, 2000). On Titan, an additional factor are the day to night winds which transport energy into the nightside. (c) Horizontal winds on Titan reach 60 (30) m/sec at solar maximum (minimum), those on Triton 3 (1) m/sec. The flow on both moons is essentially from day to night and mostly perpendicular to the isotherms (isobars), due to the balance between pressure gradients and viscosity, as discussed in 4.2. Vertical winds (not shown) reach 1.1 (0.45) m/sec on Titan during solar maximum (minimum), those on Triton 0.11 (0.03) m/sec. Vertical winds flow upward during the day and downward during night, their contours aligning well with those of the temperatures in Figure 2. These vertical winds are generated primarily by the divergence of horizontal winds and to much

lesser extent by the thermal expansion and contraction of the atmosphere. (d) The daily global temperature maximum over the equator at equinox occurs roughly one “Titan hour” after local noon on Saturn’s moon and one “Triton hour” before local noon on Neptune’s moon. The local temperature phase depends on latitude, being largest at the latitude of the sub-solar point and decreasing with distance from it. (e) Due to the larger inclination of Triton’s rotation axis and resulting larger sub-solar latitude at solstice, the summer temperature maximum on Triton occurs at higher latitude (50°) than on Titan (24°). (f) Temperatures on Titan remain fairly constant with latitude and local time on the dayside, but horizontal gradients become up to 4 times stronger at dawn, dusk and the nightside. As a result, equatorward winds on the nightside are stronger than the poleward winds on the dayside. Similarly, the day-night winds on Titan tend to accelerate when passing the terminator into the nightside.

The sharper temperature gradients on Titan’s nightside are linked to a phenomenon not found as strongly on Earth and other planets, the high latitude nightside solar heating, which is illustrated in Figure 3. The diagram is a cut through Titan (round filled center) and its thermosphere (ring) from day (right) to night (left) during equinox, the poles being located at the top and bottom. The contour levels are logs of solar volume heating rates. Values are largest over the equatorial sub-solar point and decrease towards the poles due to the larger solar zenith angles. The figure shows that heating at high latitudes extends also into the nightside. This is a result of Titan’s atmosphere being large relative to the moon’s radius and sufficiently optically thin. Due to the extended nature of the atmosphere, the nighttime shadow of Titan and its optically thick lower atmosphere has a radius of around 3000 km, while the upper thermosphere has a radius of 3900 km, 30% more. As a result of the high latitude heating, the nighttime “footprint” on the upper left panel of Figure 2 is relatively small, causing the earlier described sharper temperature gradients. On Triton, horizontal temperature gradients are more uniform throughout the day, so the winds do not show the same features as on Titan. Nevertheless, the conditions for high latitude nightside solar heating also apply on Triton. Its exosphere lies near 400 km altitude, which is 30 % of Triton’s radius, so the geometric proportions in terms of thermosphere radius and moon radius are similar as on Titan. The reason for the effect not showing up as much in the temperatures and winds of Triton is, like its smaller day-night temperature gradients, linked to the larger distance from Sun and faster rotation rate, which both reduce the efficiency of solar heating on Triton.

4.2. Balance of Forces

One of the important benefits of using GCM’s is the ability to analyze in detail the balance of forces and thus achieve a deeper understanding of the processes governing

dynamics. Figure 4 illustrates the accelerations acting upon gas particles at latitude 60N and 15:40 h local time (LT) in the exosphere on Titan (a) and Triton (b). This choice of location and local time represents an "average" case, more common than equatorial and/or noon and midnight conditions. Again, the panels represent the case driven by solar heating alone. Arrow lengths in panels a) and b) are on different scales; the pressure acceleration arrow for Titan (a) has a value of 1.6×10^{-3} m/sec^2, that for Triton (b) 4.1×10^{-4} m/sec^2. With the highest temperature on Titan during equinox occurring over the equator near 13:00 LT, pressure gradients at 60N/15:30 LT accelerate towards the north-east. These are balanced by vertical viscous drag towards the south-west. Winds at that location and time blow towards the north-east (see upper left panel of Fig. 2), so Coriolis forces are directed towards the south-east. Since winds move along a curved surface, they experience centrifugal accelerations, which are often referred to as curvature forces and in Figure 4 a) point towards the south-east. The simulations show that these forces are particularly important on Titan, while on Earth they are generally negligible. The Coriolis and curvature forces are balanced by horizontal advection. So, on Titan the primary balance of forces in the thermosphere is between pressure and viscosity as well as between curvature, Coriolis and horizontal advection. Note that geostrophy, where pressure gradients are balanced by Coriolis forces, does not hold on Titan. This is in contrast to conditions in the Earth's thermosphere, where at low to mid latitudes pressure gradients are balanced primarily by Coriolis forces and at high latitudes also by ion drag. On Triton (Figure 4 b) the pressure gradient accelerations are, as on Titan, balanced by viscosity, but curvature and advection are negligible, due to the small wind velocities. Coriolis acceleration, due to Triton's retrograde rotation, points towards the north-west, opposite to the direction on Titan. These examples illustrate that wind profiles for Titan and Triton (Figure 2) at first look very similar, but the underlying accelerations are different on both moons and different from Earth as well.

The above described the momentum balance in the thermospheres driven by solar heating alone. The inclusion of lower boundary zonal jets on Titan (see Section 5) alters the main momentum balance to occur between pressure gradients and curvature (*Müller-Wodarg et al.*, 2000), in accordance with predictions by *Rishbeth et al.* (2000). If magnetospheric coupling on Triton (see Section 5) generates larger winds in its thermosphere, the momentum balance there is expected to resemble that of Titan.

4.3. Energy Sources and Sinks

The discussions of acceleration terms in the previous section can similarly be carried out for heating terms in order to explain the global structure of temperatures on Titan and Triton (contours in Figure 2). Heating terms during equinox

conditions at solar maximum for latitude 60°N versus local time (LT) are shown in Figure 5 for Titan (a) and Triton (b). The main energy source on both moons in our simulations is solar heating (solid curves) which is zero between 22:00 (21:00) and 02:00 (03:00) h LT on Titan (Triton) and rises to a maximum at local noon. Note that solar heating persists for another 4 (3) hours into the evening sector on Titan (Triton) and starts earlier in the morning by the same amount of time This is a result of the nightside heating discussed in Section 4.1 and illustrated in Figure 3. Sunset occurs 1 hour later and sunrise one hour earlier on Titan than on Triton, but the solid curve in Figure 5 b) illustrates that nightside heating is also important on Triton. In terms of vertical structure (not shown), the solar heating curve on Titan peaks near the 10 and 0.1 nbar pressure levels, corresponding to around 750 and 1000 km altitude, with globally averaged solar maximum heating rates of 6×10^{-10} and 4×10^{-10} ergs/cm^3/sec, respectively. The lower of these peaks is primarily due to absorption of the Lyman α line (1216 Å) by CH_4, while the upper peak is caused by absorption in the He II line (304 Å) through N_2. This illustrates that both CH_4 and N_2 are important solar energy absorbers on Titan. Solar EUV heating on Triton in our simulations peaks near 180 km altitude at rate of around 9×10^{-11} ergs/cm^3/sec and is primarily due to the He II line absorption by N_2. Above 150 km, CH_4 disappears on Triton (*Strobel and Summers*, 1995), but Lyman α line absorption by CH_4 does occur in our simulations at the bottom of the thermosphere, near the 20 km altitude level, with a globally averaged rate of around 1×10^{-10} ergs/cm^3/sec.

Energy sinks on Titan are primarily the HCN rotational band cooling (narrow-dashed line in Fig. 5 a) and vertical molecular heat conduction (dotted line in Fig. 5 a). Simulations for solar maximum (minimum) conditions have shown the HCN radiative cooling to be the dominant cooling term below the 1 *p*bar (10 *p*bar) pressure level, corresponding to around 1450 (1200) km altitude, while at higher altitudes molecular conduction dominates. On Triton (Figure 5 b) molecular conduction is the principal cooling term at all heights throughout the thermosphere. Adiabatic heating and cooling (dashed-dotted lines), generated by the vertical motion of gases, also play an important role on both moons, cooling the dayside and heating nightside. As a result, the adiabatic processes contribute towards reducing the day-night temperature differences. The large magnitudes of adiabatic terms are partly due to the small moon radii. Another important factor is the large change of gravity acceleration with height. On Titan (Triton), gravity at the top of the thermosphere is only around 40 (60) % of the value at the bottom, while on Earth it is 86 % the bottom level value. This illustrates that changes of gravity with height are much more important on Titan and Triton than on Earth. Adiabatic processes were also found to play a role on Mars (see Chapter IV.1). Figure 5 illustrates that horizontal advection

(wide-dashed lines) is important on Titan, but less so on Triton, due to the smaller winds there and faster rotation rate of the moon. Energy on Titan is transported by horizontal winds from the hotter dayside into the dawn and dusk as well as night sectors, thus also contributing towards reducing the day-night temperature difference. At dawn and dusk it amounts to roughly the same value as solar heating, while on the nightside it is as strong as adiabatic heating.

These discussions have shown that dynamical terms play an important role in determining the energy distributions on Titan and Triton. Terms such as adiabatic heating and cooling as well as horizontal advection cannot be considered in 1-D models since these do not calculate vertical and horizontal winds. The use of general circulation models have enabled us for the first time to evaluate the importance of these terms on Titan and Triton.

5. DYNAMICAL AND ENERGETIC COUPLING TO OTHER REGIONS

5.1. Coupling to the Magnetosphere

Coupling to the magnetosphere can generally occur through three different processes, particle precipitation, Joule heating and ion-neutral drag. In the first, particles originating from the magnetosphere travel along the magnetic field lines and hit the atmospheric gas molecules, causing localized ionization and heating. The second is a result of electrical currents which result from convection electric fields, generated by the moving magnetospheric field lines. Both forms of heating alter pressure gradients and thereby the direction of the neutral winds. The third form of coupling consists in momentum exchange between colliding ions and neutral particles. It only plays a role when ions are constrained in their motion by strong intrinsic magnetic fields, such as that on Earth, and the Gas Giants. Titan, Triton and other weakly magnetized bodies experience only the first two forms of coupling to the magnetosphere. For a more comprehensive discussion of magnetospheric coupling, see Chapter II.

The calculations presented in Section 4 considered solar heating as the only external source of energy on Titan and Triton. By doing so, globally averaged exospheric temperatures of around 170 (50) K were achieved on Titan (Triton) for solar maximum conditions. For Titan the value is in good agreement with Voyager observations (*Smith et al.*, 1982), but for Triton it lies far below the value of 102±3 K suggested by the Voyager UVS solar occultation experiments (*Broadfoot et al.*, 1989; *Krasnopolsky et al.*, 1993). This shows that Titan's thermal structure can be understood on the basis of solar EUV and UV heating alone, while on Triton an additional energy source is needed to maintain the 102 K thermosphere. Calculations by *Stevens et al.* (1992) showed that magnetospheric power input could provide the missing energy on Triton. The moon lies within

the magnetosphere of Neptune and is exposed to energetic plasma traveling from Neptune's upper atmosphere along the magnetic field lines into the upper atmosphere of Triton. There, they cause ionization and dissociation of N_2 molecules. The generated vibrationally excited N_2 molecules collide with ionospheric electrons, thus generating translational energy, while the generated N_2^+ ions recombine and generate fast N atoms or react with H_2 to create fast H atoms. These processes generate heating at around 350 km altitude which can reach up to 20 times the solar heating rate (*Stevens et al.*, 1992). The magnetospheric heating is most effective when Triton is positioned over Neptune's magnetic equator. The 28° tilt of Neptune's rotational axis combined with the 47° tilt of its magnetic axis and Triton's 157° orbital inclination give rise to a complicated geometry of Neptune's magnetic field with respect to Triton. As Neptune rotates once every 16.1 hours and Triton once every 5.6 days, Neptune's magnetic equator crosses Triton roughly 8 times per day. Furthermore, a different side of Triton faces Neptune every time it crosses the magnetic equator, so both the intensity and global distribution of magnetospheric heating experienced on Triton will change with time. Since the heating is not distributed uniformly across the globe it will affect pressure gradients and thereby winds. Due to the complexity of the spatial distribution and time variation of these pressure gradients, the induced wind patterns will be similarly complex, with globally propagating waves. So, magnetospheric heating on Triton is likely not only to considerably affect the exospheric temperatures, but also the global winds. No calculations have so far been carried out to quantify this effect.

The impact of magnetospheric electrons from Saturn on the upper atmosphere of Titan was calculated by *Galand et al.* (1999). Their calculations suggested a magnetospheric heating rate comparable with the solar energy input. This will affect global winds as well. An interesting aspect about Titan is that it lies partly outside and partly inside Saturn's magnetosphere. When positioned between the Sun and Saturn, the solar wind pressure sufficiently pushes Saturn's magnetosphere back for Titan to lie outside the magnetosphere and exposed to the solar wind. In this scenario, no magnetospheric heating occurs on Titan. Half an orbit later Titan lies well within the magnetosphere, shielded from the solar wind but exposed to magnetospheric particles. With the solar heating being fixed in the local time frame and the magnetospheric one in the longitude frame, the two beat against each other, sometimes heating the same hemisphere and at other times the opposite ones. So, magnetospheric heating on Titan is likely to have interesting effects on the winds as well.

5.2. Coupling to the Lower Atmosphere.

The simulations discussed in Section 4 assumed zero winds at the models' lower boundaries and thus ignored any

effects of vertical coupling to lower altitudes. This coupling is important on Earth, where upwards propagating tides and planetary waves have a strong influence on the dynamics and energetics of the thermosphere (see Chapter III.1). Theoretical studies for Jupiter (*Matcheva and Strobel*, 1999; *Hickey et al.*, 2000; *Matcheva et al.*, 2001) showed that upward propagating gravity waves could explain its large exospheric temperatures. Tides are also found to affect the thermosphere of Mars (see Chapter III.1 and *Forbes and Hagan*, 2000; *Wilson*, 2000). The plausible question is thus what role this coupling to lower altitudes plays on Titan and Triton.

The presence of strong zonal jets in the stratosphere of Titan was suggested from Voyager observations by *Flasar et al.* (1981) and inferred from observations of the 28 Sgr occultation by Titan (*Hubbard et al.*, 1993). Wind speeds with peak values of up to 175 m/sec were proposed and later theoretically reproduced in calculations by *Hourdin et al.* (1995). To-date, it is unclear what happens to these jets in the 300-600 km height regime, so we do not know whether these zonal jets are still present at the base of the thermosphere. Simulations by *Müller-Wodarg et al.* (2000) have shown that the presence of such jets at the base of the thermosphere would considerably affect dynamics of the thermosphere, superimposing themselves almost linearly onto the solar-driven thermospheric winds of Figure 2. One implication of this is that wind measurements from Cassini in the thermosphere could be used to constrain dynamics at the base of the thermosphere as well, more than 350 km below the anticipated altitude of the measurements. As pointed out in Section 2.2, the presence of zonal jets was also proposed below 100 km altitude for the atmosphere of Triton (*Smith et al.*, 1989; *Hansen et al.*, 1990; *Soderblom et al.*, 1990). Since these observations provide no coherent picture no attempts were made here to simulate their effects on thermospheric dynamics. In principle, however, Triton's thermosphere should respond similarly to that of Titan.

Rishbeth et al. (2000) pointed out the possibility of gravitational semidiurnal tides on Titan. Due to the 3% eccentricity of Titan's orbit around Saturn, the gravitational pull on Titan's atmosphere varies semidiurnally. Since the same side of Titan always faces Saturn, these oscillations would be fixed in longitude. Vertical propagation of these oscillations may affect the dynamics of Titan's thermosphere. Solar tides, which are important on Earth, may also be present on Titan, but no calculations have so far been carried out to quantify them.

6. CONCLUSIONS

This chapter presented the application of general circulation models (GCM's) to the thermospheres of Titan and Triton. It showed that such models provide a deep insight into the morphology of processes, allowing to analyze the accelerations and energy balance globally.

Furthermore, they allow us to put local phenomena into a global context, which is of paramount importance when carrying out localized measurements. Finally, these models allow us to study an atmosphere under various conditions of solar activity and season, more than most measurements can cover. Nevertheless, the output from such models should be met with caution. Calculations in GCM's are carried out on the basis of fundamental equations of gas dynamics and thus "physically correct". But whether the models reproduce atmospheres realistically depends critically on the physical processes considered and the accuracy of the constraints. Discussions in Section 5 provided an example for this, showing the importance of coupling to regions above and below, which hadn't been considered in the simulations presented here. Nevertheless, there is a physical justification for omitting these processes at first, in order to understand better the complex coupled systems through separation of the different contributions. The other key factor affecting results is the accuracy of constraints. Modeling magnetospheric coupling accurately requires good knowledge of the magnetic field configuration and plasma fluxes, which in the case of Titan and Triton are yet poorly known, but Cassini measurements are anticipated to significantly improve our knowledge at least for Titan. Comparing our GCM simulations with Cassini measurements will also allow us to constrain a third contribution to thermospheric dynamics, the coupling from below. So, the use of a general circulation model for Titan's thermosphere, such as that presented here, will play an important role in the analysis of Cassini data, allowing us to potentially expand the vertical height coverage of the measurements by constraining the vertical coupling from below. Planned future extensions for the Titan GCM include self-consistent calculations of Titan's ionosphere as well.

Acknowledgments. Development of the Titan general circulation model was carried out in close collaboration with R. V. Yelle of Northern Arizona University, M. Mendillo of Boston University and A. D. Aylward of University College London (UCL). This work was funded, in part, by NSF grant AST 9816239. All calculations were carried out on the High Performance Service for Physics, Astronomy, Chemistry and Earth Sciences (HiPerSPACE) Silicon Graphics Origin 2000 supercomputer located at UCL and funded by the British Particle Physics and Astronomy Research Council (PPARC). The author wishes to thank both referees for their useful comments.

REFERENCES

Bougher, S. W., S. Engels, R. G. Roble, and B. Foster, Comparative terrestrial planet thermospheres, 2, Solar cycle variation of global structre and winds at equinox, *J. Geophys. Res.*, *104*, 16,591-16,611, 1999.

Bougher, S. W., S. Engels, R. G. Roble, and B. Foster, Comparative Terrestrial Planet Thermospheres: 3. Solar Cycle Variation of Global Structure and Winds at Solstices, *J. Geophys. Res.*, *105*, 17,669-17,689, 2000.

Broadfoot, A. L., et al., Ultraviolet spectrometer observations of Neptune and Triton, *Science*, *246*, 1459-1466, 1989.

Conrath, B., et al., Infrared observations of the Neptunian system, *Science*, *246*, 1454-1456, 1989.

Cruikshank, D. P., and P. M. Silvaggio, Triton: A satellite with an atmosphere, *Astrophys. J.*, *233*, 1016-1020, 1979.

Cruikshank, D. P., T. L. Roush, T. C. Owen, T. R. Geballe, C. de Bergh, B. Schmitt, R. H. Brown, and M. J. Bartholomew, Ices on the surface of Triton, *Science*, *261*, 742-745, 1993.

Elliot, J. L., J. A. Stansberry, C. B. Olkin, M. A. Agner, and M. E. Davies, Triton's Distorted Atmosphere, *Science*, *278*, 403-404, 1997.

Elliot, J. L., et al., Global warming on Triton, *Nature*, *393*, 765-767, 1998.

Elliot, J. L., et al., The Prediction and Observation of the 1997 July 18 Stellar Occultation by Triton: More Evidence for Distortion and Increasing Pressure in Triton's Atmosphere, *Icarus*, *148*, 347-369, 2000a.

Elliot, J. L., D. F. Strobel, X. Zhu, A. Stansberry, L. H. Waserman, and O. G. Franz, The thermal structure of Triton’s middle atmosphere, *Icarus*, *143*, 425-428, 2000b.

Forbes, J. F., and M. E. Hagan, Diurnal Kelvin Wave in the Atmosphere of Mars: Towards an Understanding of ‘Stationary’ Density Structures Observed by the MGS Accelerometer, *Geophys. Res. Lett.*, *27*, 3563-3566, 2000.

Flasar, F. M., R. E. Samuelson, and B. J. Conrath, Titan’s atmosphere: Temperature and dynamics, *Nature*, *292*, 693-698, 1981.

Friedson, A.J., and Y.L. Yung, The thermosphere of Titan, *J. Geophys. Res.*, *89*, 85-90, 1984.

Galand, M., J. Lilensten, D. Toublanc, and S. Maurice, The ionosphere of Titan: ideal diurnal and nocturnal cases, *Icarus*, *140*, 92-105, 1999.

Gurrola, E. M., E. A. Marouf, V.R. Eshleman, and G. L. Tyler, Voyager radio occultation observations of Triton’s neutral atmosphere, *Bull. Am. Astron. Soc.*, *23*, 1207, 1991.

Hanel, R., et al., Infrared observations of the Saturnian system from Voyager 1, *Science*, *212*, 192-200, 1981.

Herbert, F., and B. R. Sandel, CH_4 and haze in Triton’s lower atmosphere, *J. Geophys. Res.*, *96*, 19,241-19,252, 1991.

Hickey, M. P., R. L. Walterscheid, and G. Schubert, Gravity wave heating and cooling in Jupiter’s thermosphere, *Icarus*, *148*, 266-281, 2000.

Hourdin, F., O. Talagrand, R. Sadourny, R. Courtin, D. Gautier, and C. P. Mc Kay, Numerical simulations of the general circulation of the atmosphere of Titan, *Icarus*, *117*, 358-374, 1995.

Hubbard, W. B., et al., The occultation of 28 Sgr by Titan, *Astron.*

Astrophys., *269*, 541-563, 1993.
Ingersoll, A. P., Dynamics of Triton's atmosphere, *Nature*, *344*, 315-317, 1990.
Krasnopolsky, V. A., B. R. Sandel, and F. Herbert, Temperature, N2, and N density profiles of Triton's atmosphere: observations and model, *J. Geophys. Res.*, *98*, 3065-3078, 1993.
Lellouch, E., A. Costenis, D. Gautier, F. Raulin, N. Dubouloz, and C. Frère, Titan's atmosphere and hypothesized ocean: A reanalysis of Voyager 1 radiooccultation and IRIS 7.7-μm data, I*carus, 79,* 328-349, 1989.
Lellouch, E., Atmospheric models of Titan and Triton, *Ann. Geophys.*, *8*, 653-660, 1990.
Letourner, B., and A. Coustenis, Titan's atmospheric structure from Voyager 2 infrared spectra, *Planet. Space Sci*., *41*, 595-602, 1993.
Lindal, G. F., G. E. Wood, H. B. Hotz, D. N. Sweetnam, V. R. Eshleman, and G. L. Tyler, The atmosphere of Titan: An analysis of the Voyager 1 radio occultation measurements, *Icarus*, *53*, 348-363, 1983.
Matcheva, K. I., and D. F. Strobel, Heating of Jupiter s thermosphere by dissipation of gravity waves due to molecular viscosity and heat conduction. Icarus 140, 328 340, 1999.
Matcheva, K. I., D. F. Strobel, and F. M. Flasar, Interaction of Gravity Waves with Ionospheric Plasma: Implications for Jupiter's Ionosphere., *Icarus*, *152*, 347-365, 2001.
Müller-Wodarg, I. C. F., R. V. Yelle, M. Mendillo, L. A. Young, and A. D. Aylward, The thermosphere of Titan simulated by a global three-dimensional time-dependent model, *J. Geophys. Res.*, *105*, 20,833-20,856, 2000.
Müller-Wodarg, I. C. F., and R. V. Yelle, The Effect of Dynamics on the Composition of Titan's Upper Atmosphere, submitted to *Geophys. Res. Lett.*, 2001.
Olkin, C. B., et al., The thermal structure of Triton's atmosphere: Results from the 1993 and 1995 occultations, *Icarus*, *129*, 178-201, 1997.
Owen, T. C., T. L. Rousch, D. P. Cruikshank, J. L. Elliot, L. A. Young, C. de Bergh, B. Schmitt, T. R. Geballe, R. H. Brown, and M. J. Bertholomew, Surface ices and the atmospheric composition of Pluto, *Science*, *261*, 745-748, 1993.
Rishbeth, H., R. V. Yelle, and M. Mendillo, Dynamics of Titan's thermosphere, *Planet. Space Sci.*, *48*, 51-58, 2000.
Sicardy, B., et al., Structure of Triton's atmosphere from the occultation of Tr176, *Bull. Am. Astron. Soc.*, *30*, 1107, 1998.
Smith, G. R., D. F. Strobel, A. L. Broadfoot, B. R. Sandel, D. E. Shemansky, and J. B. Holberk, Titan's upper atmosphere: Composition and temperature from the EUV solar occultation results, *J. Geophys. Res.*, *87*, 1351-1359, 1982.
Smith, B. A., et al., Voyager 2 at Neptune: Imaging science results, *Science*, *246*, 1422-1449, 1989.
Soderblom, L. A., S. W. Kieffer, T. L. Becker, R. H. Brown, A. F. Cook II, C. J. Hansen, T. V. Johnson, R. L. Kirk, and E. M Shoemaker, Triton's geyser-like plumes: Discovery and basic characterization, *Science*, *250*, 410-415, 1990.
Stevens, M. H., D. F. Strobel, M. E. Summers, and R. V. Yelle, On the thermal structure of Triton's thermosphere, *Geophys. Res. Lett.*, *19*, 669-672, 1992.
Strobel, D. F., M. E. Summers, F. Herbert, and B. Sandel, the photochemistry of methane in the atmosphere of Triton, *Geophys. Res. Lett.*, *17*, 1729-1732, 1990.

Strobel, D.F, M.E. Summers, and X. Zhu, Titan's upper atmosphere: Structure and ultraviolet emmissions, *Icarus*, *100*, 512-526, 1992.

Strobel, D. F., and M. E. Summers, Triton's upper atmosphere and ionosphere, in *Neptune and Triton*, edited by D. P. Cruikshank, pp. 1107-1148, Univ. of Arizona Press, Tucson, 1995.

Strobel, D. F., X. Zhu, M. E. Summers, and M. H. Stevens, On the vertical thermal structure of Pluto's atmosphere, *Icarus*, *120*, 266-289, 1996.

Trafton, L., Large seasonal variations on Triton, *Icarus*, *58*, 312-324, 1984.

Vervack, R. J., B. R. Sandel, and D. F. Strobel, First results from a reanalysis of the Voyager 1 ultraviolet spectrometer solar occultation by Titan, submitted to *Icarus*, 2001.

Wilson, R. J., Evidence for diurnal period Kelvinwaves in the martian atmosphere from Mars Global Surveyor TES data, *Geophys. Res. Lett.*, *27*, 3563-3566, 2000.

Yelle, R.V., Non-LTE models of Titan's upper atmosphere, *Astrophys. J. 383*, 380-400, 1991.

Yelle, R. V., J. I. Lunine, and D. M. Hunten, Energy balance and plume dynamics in Triton's lower atmosphere, *Icarus 89*, 347-358, 1991.

Yelle, R. V., J. I. Lunine, J. B. Pollack, and R. H. Brown, Lower atmospheric structure and surface-atmosphere interactions on Triton, in *Neptune and Triton*, edited by D. P. Cruikshank, pp. 1031-1105, Univ. of Arizona Press, Tucson, 1995.

Yelle, R. V., E. Lellouch, D. Gautier, and D. F. Strobel, Engineering models for Titan's atmosphere, in *Huygens Science Payload and Mission, Eur. Space Agency Sci. Tech. Rep., ESA SP-1177*, 243-256, 1997.

Yung, Y. L., M. Allen, and J. P. Pinto, Photochemistry of the atmosphere of Titan: comparison between model and observations, *Astrophys. J. Suppl.*, *55*, 465-506, 1984.

I. C. F. Müller-Wodarg, Atmospheric Physics Laboratory, University College London, 67-73 Riding House Street, London W1P 7PP, U.K.

FIGURE AND TABLE CAPTIONS

Figure 1. The change of sub-solar latitude between 1975 and 2010 for Titan (a) and Triton (b). Also shown are seasons, times of key observations and levels of solar activity.

Figure 2. Exospheric solar-driven temperatures and horizontal winds on Titan (left panels) and Triton (right panels), as calculated by general circulation models for equinox conditions (upper row) and southern hemisphere solstice (lower row). The equinox simulations are for solar maximum, the solstice ones for solar minimum.

Figure 3. Illustration of the high-latitude nightside heating for the case of Titan. The diagram shows a day-night cut through the thermosphere (ring shaped) at equinox condition. Contours are solar volume heating rates for solar maximum. Note the heating of high latitudes at night due to the small size of the nighttime shadow cast by the moon (filled circle) and its optically thick atmosphere.

Figure 4. Horizontal acceleration terms in the exosphere at 60°N, 15:40 h local time on Titan (a) and Triton (b) during equinox conditions. North points up, east towards the right. The pressure arrow has a value of 1.6×10^{-3} m/sec^2 for Titan and 4.1×10^{-4} m/sec^2 for Triton.

Figure 5. Heating and cooling terms in the exosphere at 60°N versus local time on Titan (a) and Triton (b). Simulations are for equinox conditions at solar maximum. Rates are given in units of ergs/cm^3/sec.

Table 1. Fundamental parameters distinguishing the general circulation models of Titan and Triton used in this study.

Figure 1. The change of sub-solar latitude between 1975 and 2010 for Titan (a) and Triton (b). Also shown are seasons, times of key observations and levels of solar activity.

Figure 2. Exospheric solar-driven temperatures and horizontal winds on Titan (left panels) and Triton (right panels), as calculated by general circulation models for equinox conditions (upper row) and southern hemisphere solstice (lower row). The equinox simulations are for solar maximum, the solstice ones for solar minimum.

Figure 3. Illustration of the high-latitude nightside heating for the case of Titan. The diagram shows a day-night cut through the thermosphere (ring shaped) at equinox condition. Contours are solar volume heating rates for solar maximum. Note the heating of high latitudes at night due to the small size of the nighttime shadow cast by the moon (filled circle) and its optically thick atmosphere.

Figure 4. Horizontal acceleration terms in the exosphere at 60°N, 15:40 h local time on Titan (a) and Triton (b) during equinox conditions. North points up, east towards the right. The pressure arrow has a value of 1.6×10^{-3} m/sec^2 for Titan and 4.1×10^{-4} m/sec^2 for Triton.

Figure 5. Heating and cooling terms in the exosphere at 60°N versus local time on Titan (a) and Triton (b). Simulations are for equinox conditions at solar maximum. Rates are given in units of ergs/cm^3/sec.

Table 1: Fundamental parameters distinguishing the general circulation models of Titan and Triton used in this study.

THE THERMOSPHERES OF TITAN AND TRITON

I. C. F. MÜLLER-WODARG

Parameter	Titan	Triton
Radius	2575 km	1353 km
Sun distance	9.5 AU	30.5 AU
Pressure range	0.1 μbar - 1 *p*bar	1 μbar - 0.01 *p*bar
Height range	600 - ca. 1400 km	10 - ca. 420 km
Gravity at bottom	0.89 ms^{-2}	0.75 ms^{-2}
Rotation rate (duration of day) and orientation	4.6×10^{-6} s^{-1} (15.8 days)	-1.3×10^{-5} s^{-1} (5.6 days)
Max. subsolar latitude	$\lambda_{max} = 24°$	$\lambda_{max} = 50°$
Mixing ratios	*Yung et al.* [1984]	99.99 % N_2; 0.01 % CH_4

Table 1

Figure 1

a)

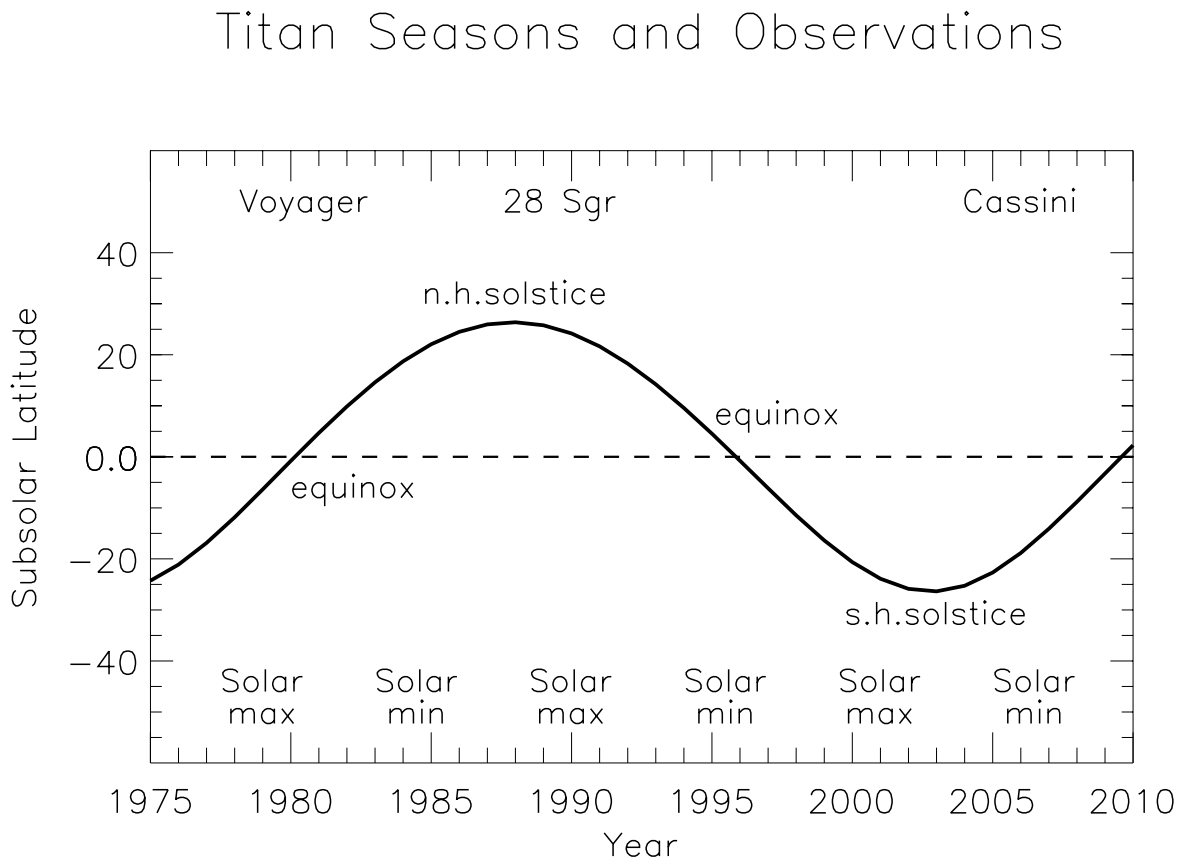
Titan Seasons and Observations
Voyager
28 Sgr
Cassini
40
20
0.0
−20
−40
n.h.solstice
equinox
equinox
s.h.solstice
Solar max
Solar min
Solar max
Solar min
Solar max
Solar min
Subsolar Latitude
1975
1980
1985
1990
1995
2000
2005
2010
Year

Figure 1

b)

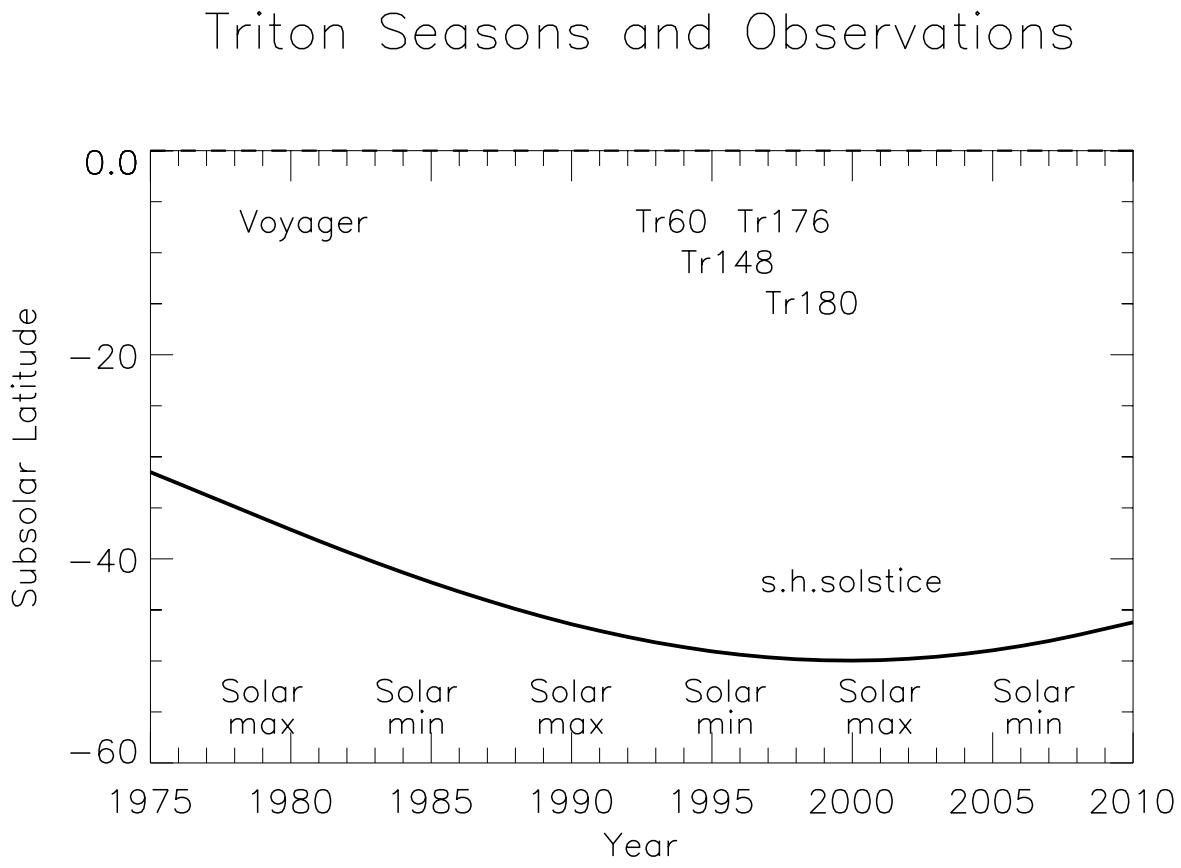
Triton Seasons and Observations
0.0
−20
−40
−60
Subsolar Latitude
Voyager
Tr60 Tr176
Tr148
Tr180
s.h.solstice
Solar max
Solar min
Solar max
Solar min
Solar max
Solar min
1975
1980
1985
1990
1995
2000
2005
2010
Year

Figure 2

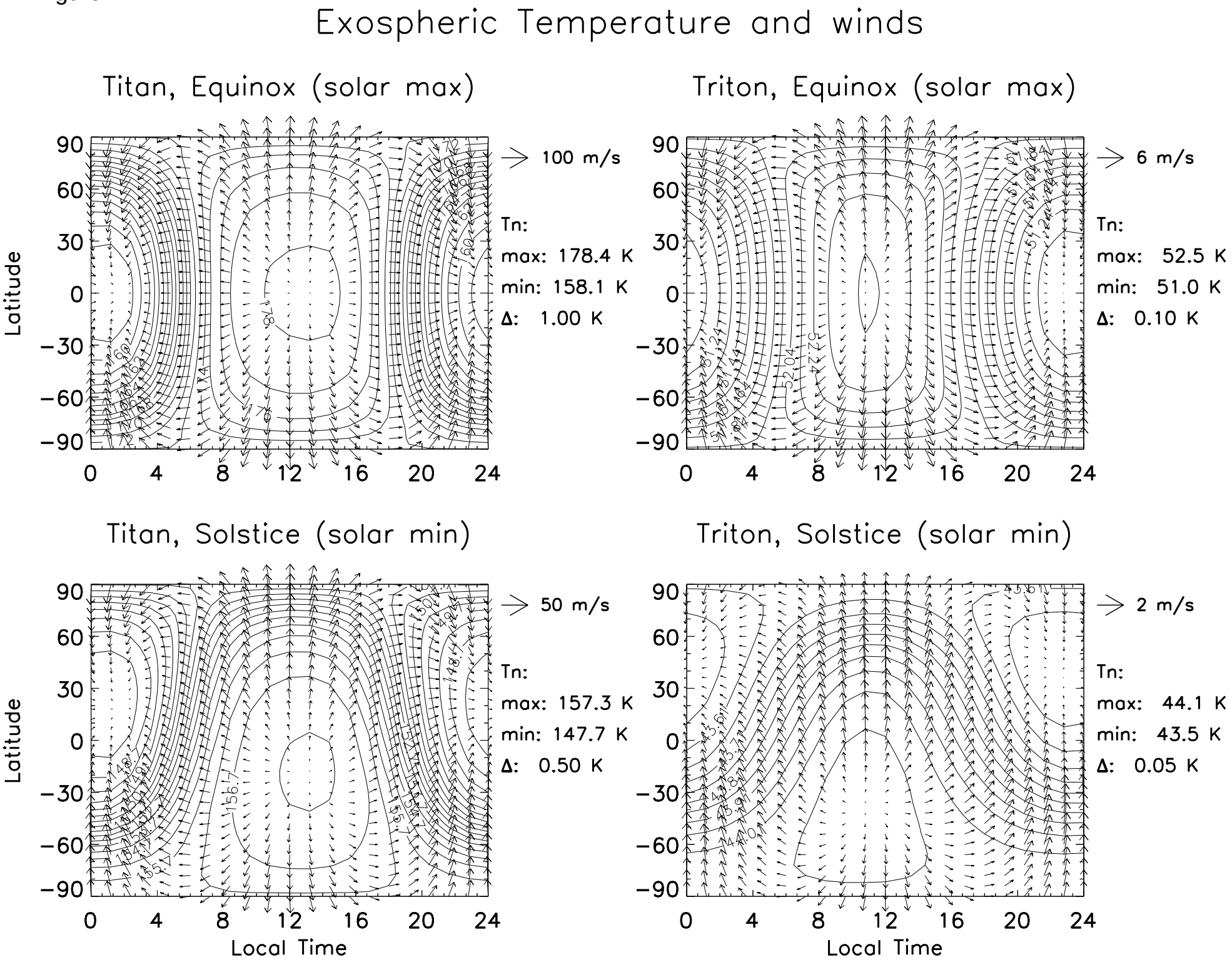
Exospheric Temperature and winds
Titan, Equinox (solar max)
100 m/s
Tn:
max: 178.4 K
min: 158.1 K
Δ: 1.00 K
Triton, Equinox (solar max)
6 m/s
Tn:
max: 52.5 K
min: 51.0 K
Δ: 0.10 K
Titan, Solstice (solar min)
50 m/s
Tn:
max: 157.3 K
min: 147.7 K
Δ: 0.50 K
Triton, Solstice (solar min)
2 m/s
Tn:
max: 44.1 K
min: 43.5 K
Δ: 0.05 K
Latitude
Local Time
90
60
30
0
−30
−60
−90
0
4
8
12
16
20
24

Figure 3

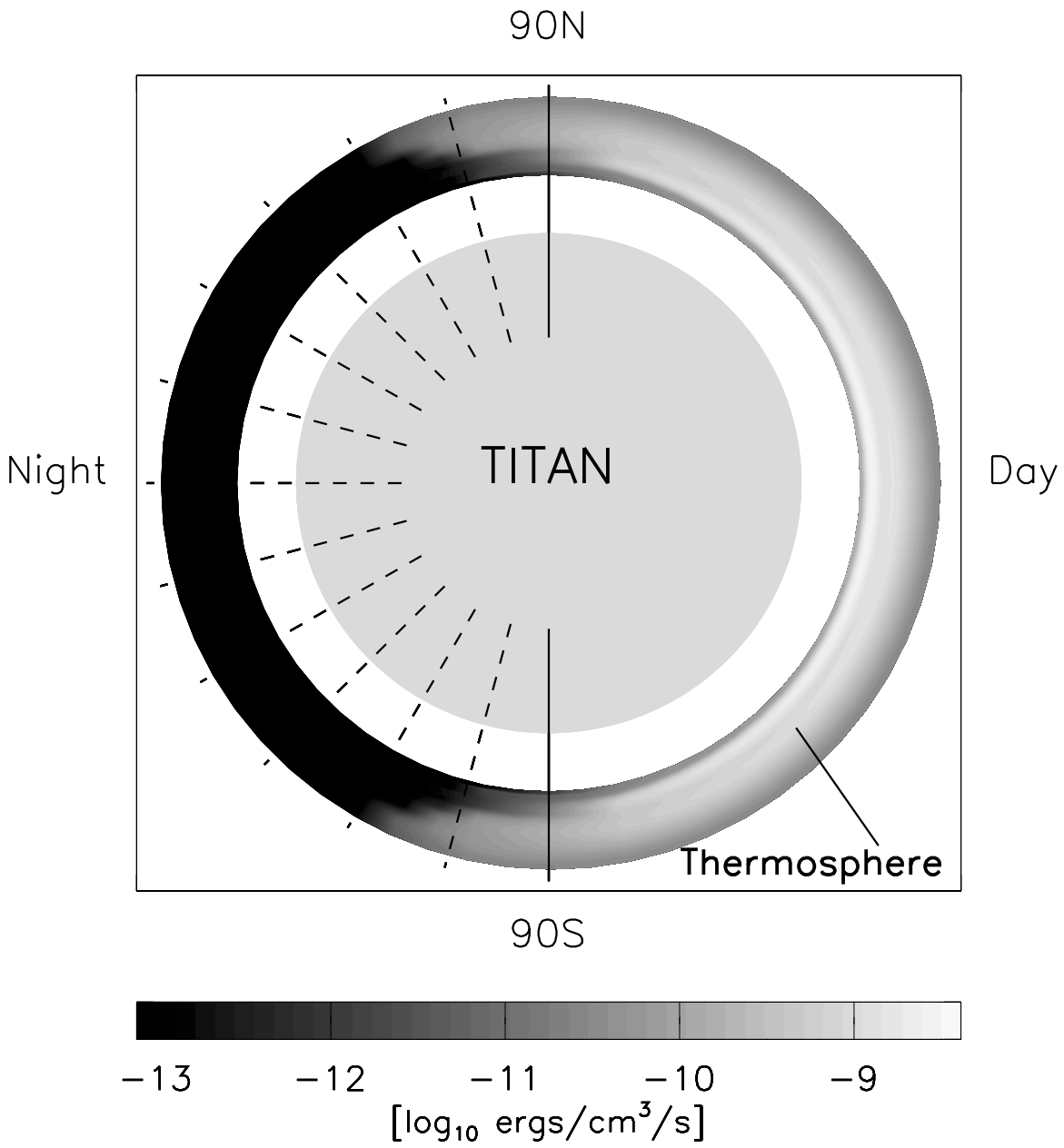
90N
Night
TITAN
Day
Thermosphere
90S
−13
−12
−11
−10
−9
[log10 ergs/cm3/s]

Figure 4
a)

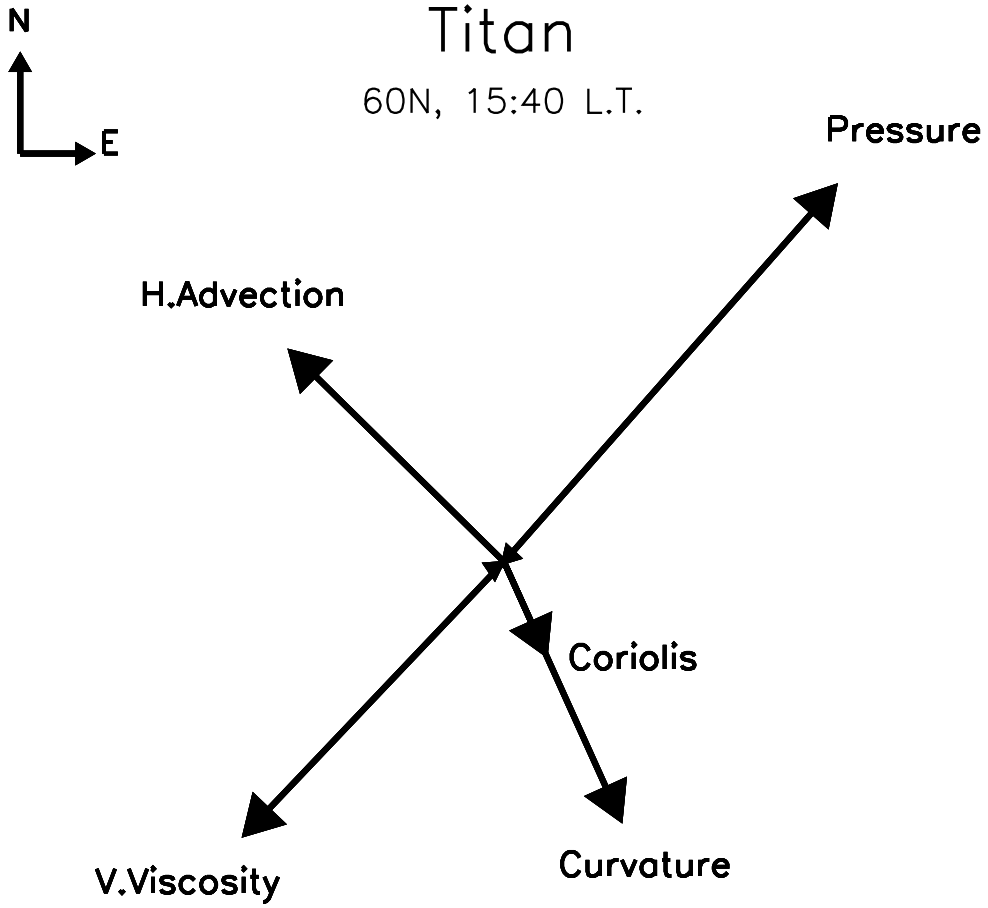
N
E
Titan
60N, 15:40 L.T.
Pressure
H.Advection
Coriolis
V.Viscosity
Curvature

Figure 4
b)

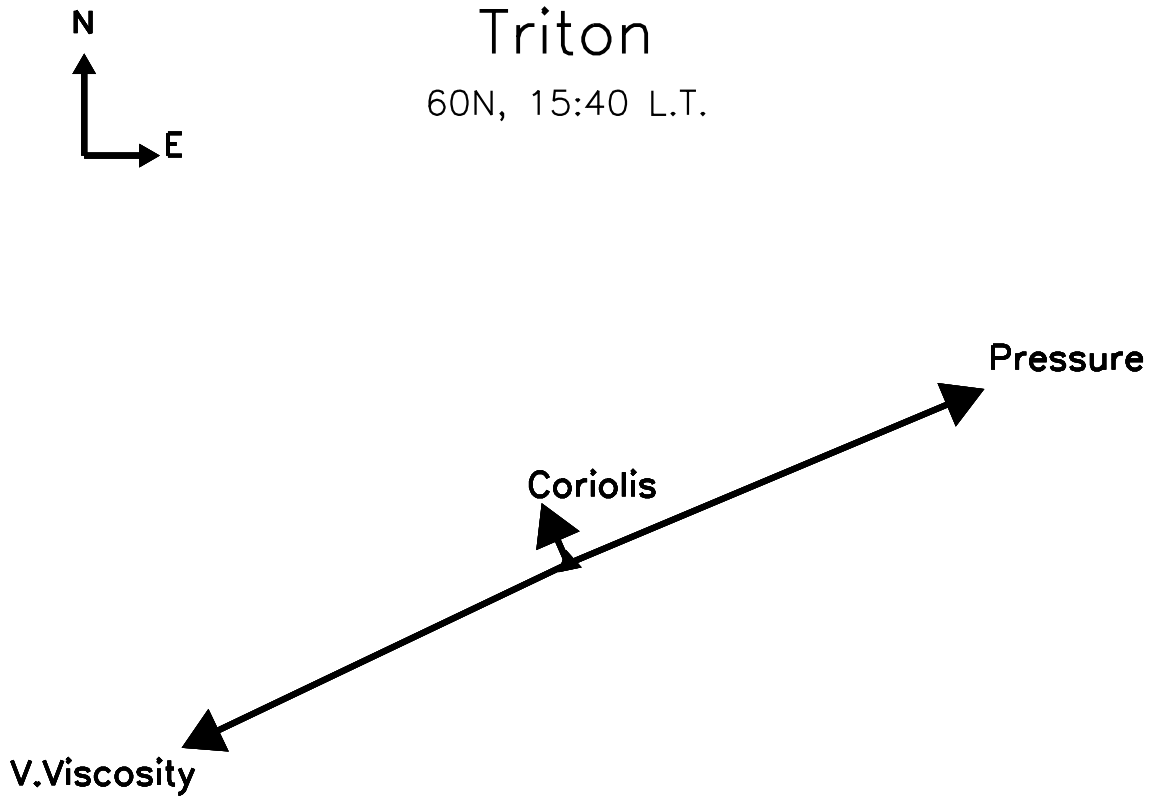

Figure 5

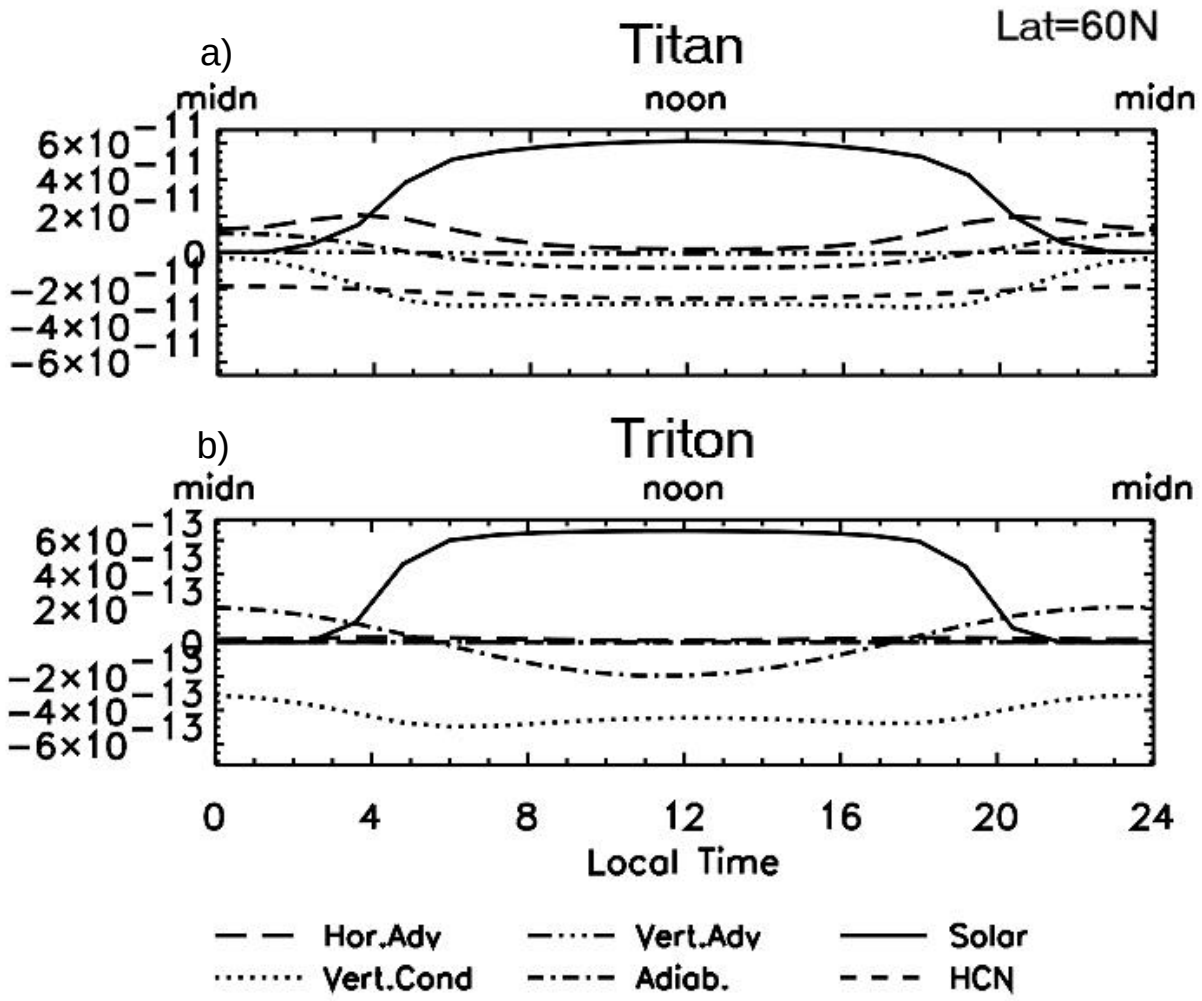
a)
Titan
Lat=60N
midn
noon
midn
6×10⁻¹¹
4×10⁻¹¹
2×10⁻¹¹
0
−2×10⁻¹¹
−4×10⁻¹¹
−6×10⁻¹¹
b)
Triton
midn
noon
midn
6×10⁻¹³
4×10⁻¹³
2×10⁻¹³
0
−2×10⁻¹³
−4×10⁻¹³
−6×10⁻¹³
0
4
8
12
16
20
24
Local Time
Hor.Adv
Vert.Adv
Solar
Vert.Cond
Adiab.
HCN